

**Two isostructural Ln³⁺-based heterometallic MOFs for the detection
of nitro-aromatic and Cr₂O₇²⁻**

Yuxiao Zhang, Yiting Ying, Meng Feng, Liang Wu, Dongmei Wang and Chunxia Li**

*Key Laboratory of the Ministry of Education for Advanced Catalysis Materials,
College of Chemistry and Life Sciences, Zhejiang Normal University, Jinhua 321004,
P. R. China. E-mail: dmwang@zjnu.edu.cn, cxli@zjnu.edu.cn.*

Calculation procedures of fluorescence quenching efficiency

The fluorescence quenching efficiency of **In/Eu-CBDA** and **In/Tb-CBDA** can be evaluated by the Stern-Volmer constant (K_{sv}), which is calculated by using the Stern-Volmer equation:

$$I_0/I = 1 + K_{sv}[M]$$

(I_0 = the initial luminescence intensity, I = the luminescence intensity after the addition of the analytes, $[M]$ = the concentration of the analytes and K_{sv} = the Stern-Volmer constant).

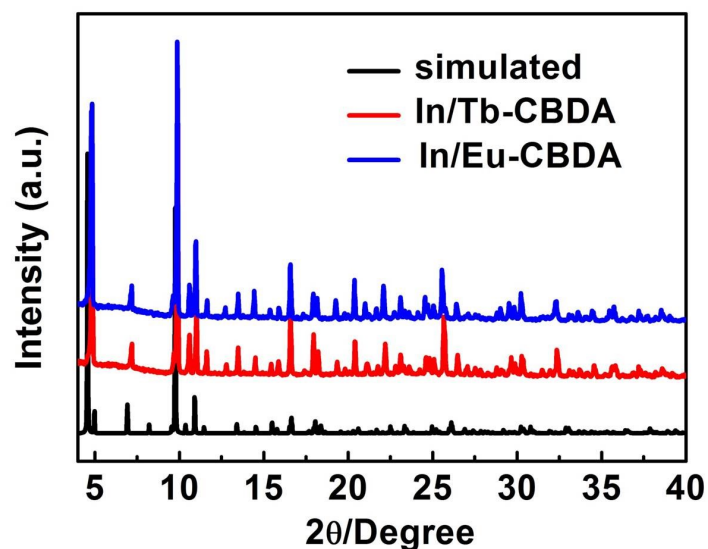


Fig. S1 Powder XRD spectra of **In/Tb-CBDA**, **In/Eu-CBDA** and single crystal structures.

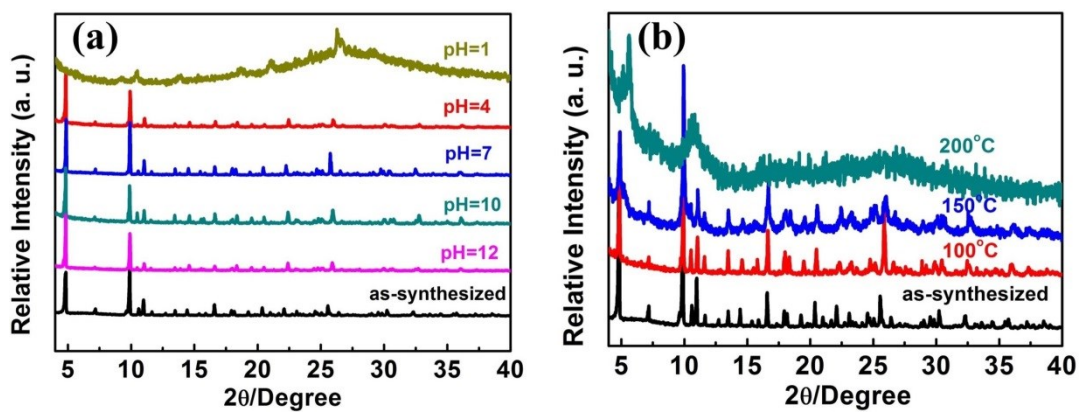


Fig. S2 PXRD patterns for **In/Eu-CBDA** samples (a) at different pH and (b) at variable temperatures.

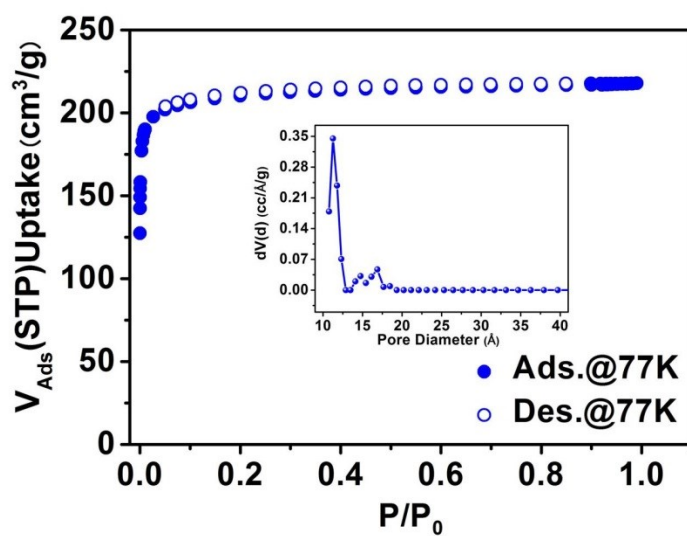


Fig. S3 Sorption isotherm and pore size distribution of **In/Eu-CBDA** at 77 K.

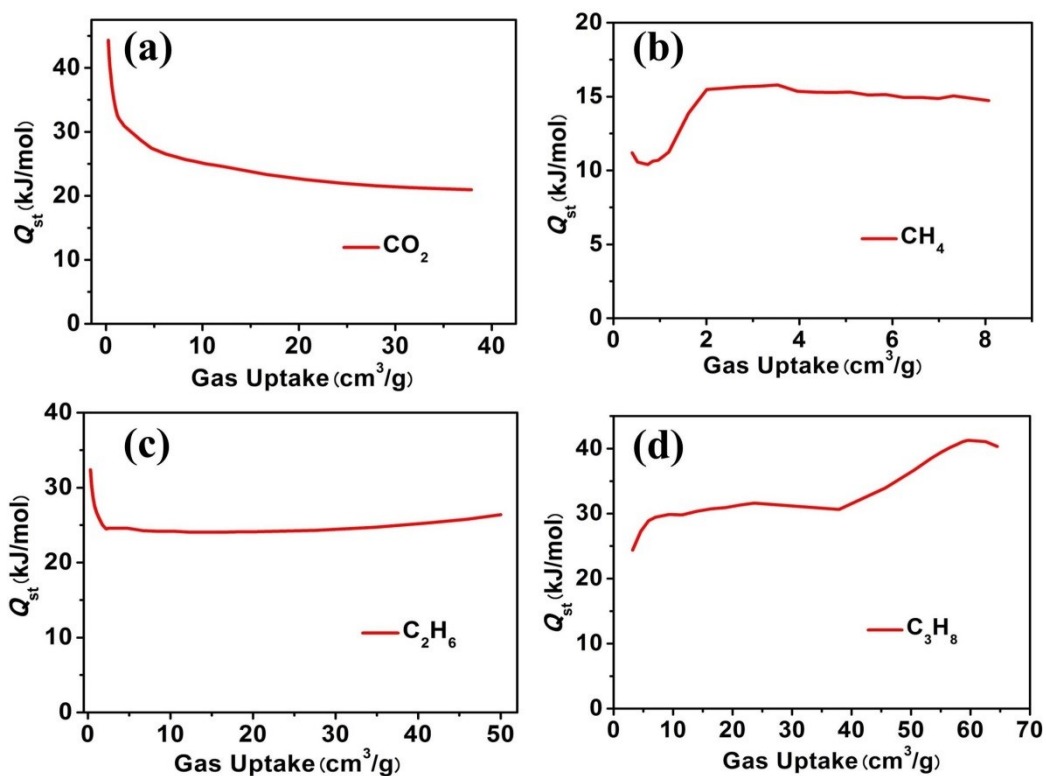


Fig. S4 Isosteric heat of CO_2 (a), CH_4 (b), C_2H_6 (c), and C_3H_8 (d) for **In/Eu-CBDA**.

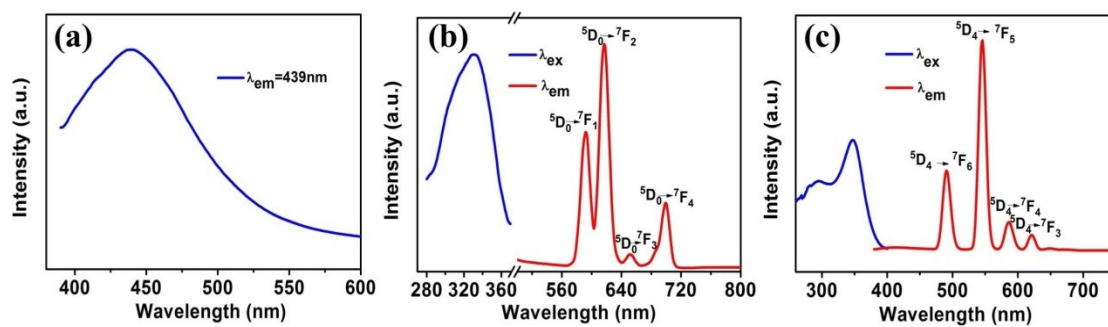


Fig. S5 Excitation and emission spectra of (a) CBDA (b) **In/Eu-CBDA** and (c) **In/Tb-CBDA**.

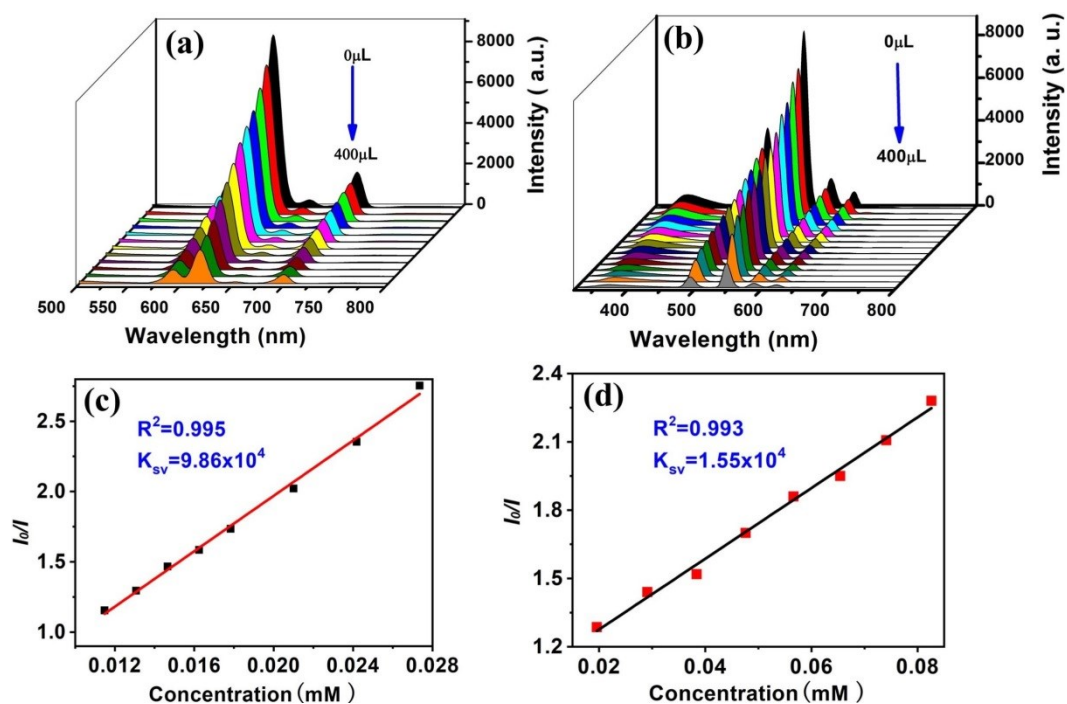


Fig. S6 (a) and (b) are the fluorescence spectra of 1,4-dinitrobenzene for **In/Eu-CBDA** and **In/Tb-CBDA** at different concentrations; (c) and (d) are the Stern-Volmer (SV) spectrum of 1,4-dinitrobenzene for **In/Eu-CBDA** and **In/Tb-CBDA**.

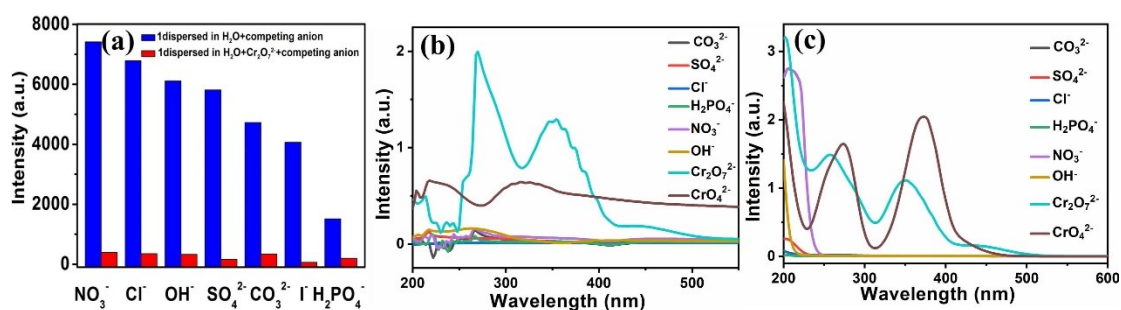


Fig. S7 (a) Fluorescence intensity spectrogram of **In/Tb-CBDA** in aqueous solution containing different competing ions and fluorescence intensity spectrum after adding $\text{Cr}_2\text{O}_7^{2-}$. UV-Vis absorption spectra of (b) **In/Eu-CBDA** and (c) **In/Tb-CBDA** in DMF solutions with different potassium anions.

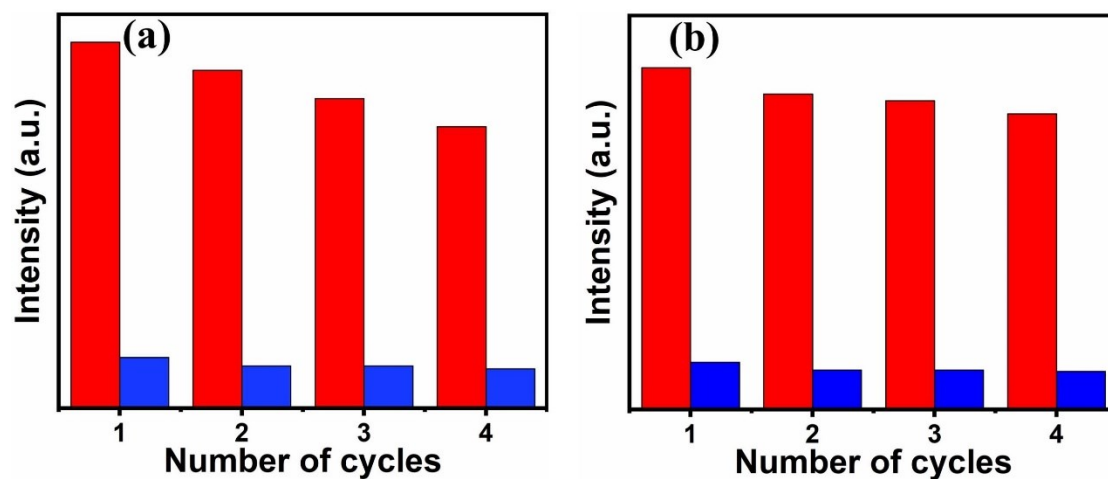


Fig. S8 The reproducibility of the quenching ability of (a) **In/Eu-CBDA** and (b) **In/Tb-CBDA** on $\text{Cr}_2\text{O}_7^{2-}$.

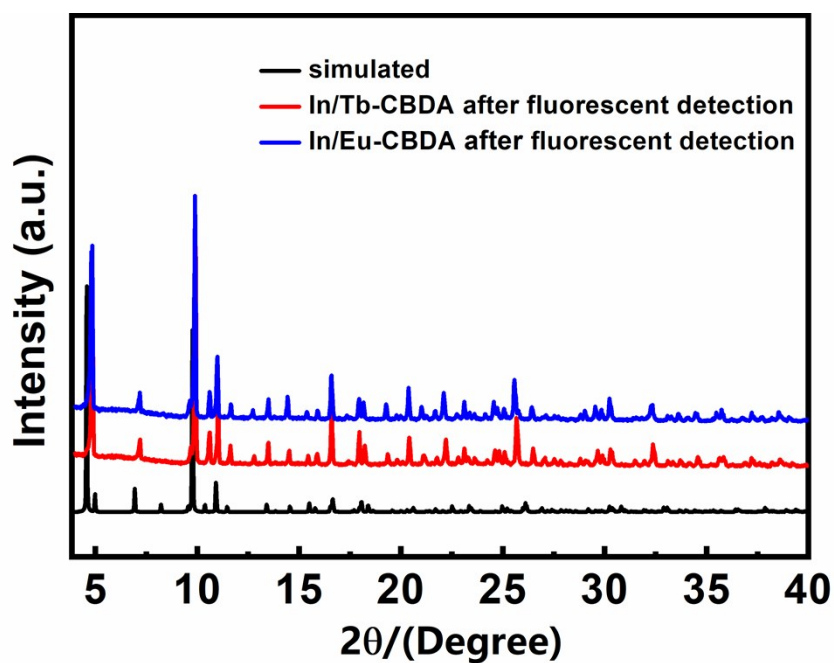


Fig. S9 The powder XRD patterns for **In/Eu-CBDA** and **In/Tb-CBDA** after fluorescent detection.

Table S1 Comparison of detection ability on representative MOFs towards Cr₂O₇²⁻.

Materials	Ksv (M ⁻¹)	Detection limit (ppb)	Solvent	Reference
In/Eu-CBDA	1.08×10 ⁴	2.15×10 ⁸	DMF	This work
In/Tb-CBDA	1.72×10 ⁴	8.72×10 ⁶	water	This work
Zn-MOF-1	2.07×10 ⁴	3.53×10 ⁶	water	[1]
[Zn ₂ (TPOM)(NH ₂ -BDC) ₂]·4H ₂ O	7.59×10 ³	3.90×10 ⁶	DMF	[2]
[Cd(L)(TPOM) _{0.75}]·xS	1.35×10 ⁴		water	[3]
[Zn(L)(BBI)·(H ₂ O) ₂]	1.17×10 ⁴		water	[3]
[Eu(Hpzbc) ₂ (NO ₃) ₃]·H ₂ O		2.20×10 ⁷	ethanol	[4]
[Zn ₂ (TPOM)(NDC) ₂]·3.5H ₂ O	9.21×10 ³	2.35×10 ⁶	water	[5]
534-MOF-Tb	1.37×10 ⁴	1.40×10 ⁸	water	[6]
Eu ³⁺ @MIL-121	4.34×10 ³	5.40×10 ⁴	water	[7]
[Zn ₇ (TPPE) ₂ (SO ₄ ²⁻) ₇](DMF·H ₂ O)	1.09×10 ⁴	26.98	water	[8]
[Tb(TATAB)(H ₂ O) ₂]·NMP	1.11×10 ⁴		water	[9]
[Zn ₃ (tza) ₂ (μ ₂ -OH) ₂ (H ₂ O) ₂]H ₂ O	5.02×10 ³	1.00×10 ⁶	water	[10]
[Zn(btz)] _n	3.19×10 ³	5.20×10 ²	water	[11]
[Zn ₂ (tz)H ₂ O] _n	2.19×10 ³	1.04×10 ³	water	[11]
[Eu(ipbp) ₂ (H ₂ O) ₃]Br·6H ₂ O	8.98×10 ³	5.16×10 ⁹	water	[12]
[Eu ₇ (mtb) ₅ (H ₂ O) ₁₆]·NO ₃ ·8DMA·18H ₂ O	3.34×10 ⁴	0.56	water	[13]
[Zn ₃ (bpanth)(oba) ₃]·2DMF	9.40×10 ⁴	7.00×10 ²	water	[14]
Zr ₆ O ₄ (OH) ₇ (H ₂ O) ₃ (BTBA) ₃	1.57×10 ⁴	1.50×10 ⁶	water	[15]

- (1) X.-Y. Guo, F. Zhao, J.-J. Liu, Z.-L. Liu and Y.-Q. Wang, *J. Mater. Chem. A*, 2017, **5**, 20035-20043.
- (2) R. Lv, J. Wang, Y. Zhang, H. Li, L. Yang, S. Liao, W. Gu and X. Liu, *J. Mater. Chem. A*, 2016, **4**, 15494-15500.
- (3) Y. Zhao, X. Xu, L. Qiu, X. Kang, L. Wen and B. Zhang, *ACS Appl Mater. Interfaces*, 2017, **9**, 15164-15175.
- (4) G.-P. Li, G. Liu, Y.-Z. Li, L. Hou, Y.-Y. Wang and Z. Zhu, *Inorg. Chem.*, 2016, **55**, 3952-3959.
- (5) R. Lv, H. Li, J. Su, X. Fu, B. Yang, W. Gu and X. Liu, *Inorg. Chem.*, 2017, **56**, 12348-12356.
- (6) M. Chen, W.-M. Xu, J.-Y. Tian, H. Cui, J.-X. Zhang, C.-S. Liu and M. Du, *J. Mater. Chem. C*, 2017, **5**, 2015-2021.
- (7) J.-N. Hao and B. Yan, *New J. Chem.*, 2016, **40**, 4654-4661.
- (8) X.-X. Wu, H.-R. Fu, M.-L. Han, Z. Zhou and L.-F. Ma, *Cryst. Growth Des.*, 2017, **17**, 6041-6048.
- (9) G.-X. Wen, M.-L. Han, X.-Q. Wu, Y.-P. Wu, W.-W. Dong, J. Zhao, D.-S. Li and L.-F. Ma, *Dalton Trans.*, 2016, **45**, 15492-15499.

- (10) T.-Q. Song, J. Dong, H.-L. Gao, J.-Z. Cui and B. Zhao, *Dalton Trans.*, 2017, **46**, 13862-13868.
- (11) C.-S. Cao, H.-C. Hu, H. Xu, W.-Z. Qiao and B. Zhao, *CrystEngComm*, 2016, **18**, 4445-4451.
- (12) C. Zhang, L. Sun, Y. Yan, H. Shi, B. Wang, Z. Liang and J. Li, *J. Mater. Chem. C*, 2017, **5**, 8999-9004.
- (13) W. Liu, Y. Wang, Z. Bai, Y. Li, Y. Wang, L. Chen, L. Xu, J. Diwu, Z. Chai and S. Wang, *ACS Appl Mater. Interfaces*, 2017, **9**, 16448-16457.
- (14) Z.-Q. Yao, G.-Y. Li, J. Xu, T.-L. Hu and X.-H. Bu, *Chem. Eur. J.*, 2018, **24**, 3192-3198.
- (15) T. He, Y.-Z. Zhang, X.-J. Kong, J. Yu, X.-L. Lv, Y. Wu, Z.-J. Guo and J.-R. Li, *ACS Appl Mater. Interfaces*, 2018, **10**, 16650-16659.